SMAR 2019 – Fifth Conference on Smart Monitoring,
Assessment and Rehabilitation of Civil Structures

SMAR 2019

Bond behaviour of ribbed near-surface mounted iron-based shape memory alloy bars: Experimental investigation

Bernhard SCHRANZ [1,2], Moslem SHAHVERDI [1,3], Christoph CZADERSKI [1]

[1] Structural Engineering Laboratory, Empa, Dübendorf, Switzerland

[2] Institute of Structural Engineering (IBK), ETH, Zürich, Switzerland

[3] School of civil engineering, University of Tehran, Tehran, Iran

Contact e-mail: bernhard.schranz@empa.ch

ABSTRACT: The use of iron-based shape memory alloy (Fe-SMA), so-called "memory steel" elements for strengthening of existing concrete structures has high potential for being a competitive option to established methods. The prestressing function is obtained by activating the shape memory effect - that is, the ability of the material to return to its original shape after deformation, when heated. If the SMA element is restrained on a structure when heated, stresses will developed in the element and consequently also in the structure.
The underlying idea of the current investigation is to mount ribbed Fe-SMA bars into grooves in the cover of concrete elements with a cementitious mortar, which is called near-surface mounted (NSM) strengthening technique. In the current study, the bond behaviour of NSM Fe-SMA bars was investigated by means of pull-out tests. The aim was to study the influence of the groove dimensions and to find an optimal configuration, which could be used in a real application. The obtained average bond stress - slip behaviour can furthermore be implemented in analytical and numerical calculations.
Specimens consisted of concrete cubes, where grooves were cut into one surface and Fe-SMA bars were embedded to, on a bond-length of five times the bar diameter. The Fe-SMA bars were then subjected to tensile loading, i.e. pull out load. The design of the experiments was based on RILEM specifications. Besides pull-out load and end-slip, full-field deformations were measured with a 3D digital image-correlation system (DIC). The tests delivered satisfying results in terms of load capacity and slip. Two main failure modes were identified, which were either based on shearing of the mortar substrate adjacent to the ribs, or splitting of the cover and surrounding concrete. It was also found that the groove depth and therefore the cover thickness highly affect the bond capacity and mode of failure. The groove width did not influence either the load capacity or the slip significantly. In general, near-surface mounted Fe-SMA bars show sufficient bond performance for the use as a structural strengthening method.

1 INTRODUCTION

Well-established retrofitting procedures for deficient concrete structures include the application of non-prestressed carbon-fiber reinforced polymer (CFRP) strips, bonded to concrete with epoxy resin (Meier 1995). This measure mainly increases the ultimate load capacity within ultimate limit state design. When existing cracks and deformations are to be reduced to improve the serviceability limit state design, the CFRP elements have to be prestressed. However, most

of the CFRP applications are still non-prestressed due to the high cost of prestressed variants. Especially on smaller buildings, prestressed CFRP strengthening cannot be used economically.

A novel iron-based shape memory alloy (Fe-SMA), also known as "memory-steel", developed at the Swiss Federal Laboratories for material science and technology (Empa) in Switzerland, can be used as an alternative material for prestressed strengthening of engineering structures (Czaderski et al. 2014). The so-called shape memory effect, the ability of this material to return to its original shape after deformation, when heated, allows simple and cost-effective prestressing of concrete or metallic structures. The prestressing function is obtained, when a memory steel element is firstly deformed, then fixed to the building component, followed by heating and cooling to room temperature. During this so-called activation of the alloy, stresses are developed in the Fe-SMA element through a change in lattice structure (Lee et al. 2015). Several investigations have already proven the function of Fe-SMA strengthening of concrete structures (Shahverdi et al. 2016, Shahverdi et al. 2016, Michels et al. 2017, Michels et al. 2018, Shahverdi et al. 2018) as well as steel structures (Izadi et al. 2017). The material can be produced in the form of strips with a thickness of 1.5 mm (Shahverdi et al. 2018) and in the form of standard-geometry reinforcement bars (Michels et al. 2018, Schranz 2019) by the company re-fer AG from Brunnen, Switzerland (2019). A number of successful site-applications have already been completed and are explained in (Schranz 2019). The investigation presented herein is one of the first, using ribbed Fe-SMA bars in a strengthening application. The idea is to strengthen concrete members in a near-surface mounted (NSM) configuration, as illustrated in Figure 1. In this method, Fe-SMA bars are inserted into grooves in the concrete cover and bonded with a cementitious mortar. The near-surface mounted configuration offers better bond properties, protection against environmental influences, fire and vandalism than externally bonded methods. The required grooves can be cut with a diamond-saw. This method was firstly used in 1949, where conventional, non-prestressed steel bars were used to strengthen a concrete bridge deck (Asplund 1949). Nowadays, mainly FRP bars have been used in a NSM configuration due to higher corrosion resistance when compared to standard reinforcement bars in a low concrete cover environment (Sena-Cruz et al. 2016). The disadvantage with this method is that prestressing of NSM FRP bars is a very complex task and only used for research purposes (Lee et al. 2017) at the moment. The prestressing of NSM Fe-SMA bars or strips by activation of the shape-memory effect however is simpler due to absence of hydraulic jacks or mechanical fixations (Abouali et al. 2019).

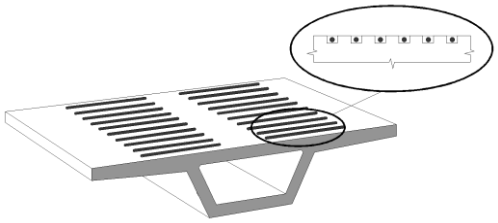

Figure 1. NSM Fe-SMA bar strengthening of a bridge-section

Common ways to investigate the bond behavior of reinforcement bars in concrete are pull-out tests. The bond behavior of conventional steel bars has been investigated for decades using full or reduced bond length. However differences of the memory steel in elastic modulus, mortar, as well as the presence of heating and prestress in combination with small cover depth require new investigations. In this study, the bond behavior of NSM Fe-SMA bars is examined by pull-out test with reduced bond length (ASTM C234 1991, RILEM TC 1994). Tests with reduced bond length are often used for parametric studies or to investigate the local bond stress-slip behavior and to calibrate bond models. The underlying assumption for such bond tests is, that if the bond-length is limited to a maximum of five times the bar diameter, a constant bond stress along the bond length can be assumed and the test would resemble the so-called incremental bond element (Rehm 1961). Due to inhomogeneity of the concrete/ mortar and local inconsistencies, shorter bond lengths are not considered practical (Windisch 1985). The RILEM pull-out test design

(RILEM TC 1994) has often been used as a base for design of bond tests with short bond length. However, concerns regarding disadvantages of this standard test have been raised before and modified approaches were proposed for example in (Windisch 1985, De Lorenzis et al. 2002).
The experimental investigations presented in this paper are part of a larger test campaign, examining the bond behavior of NSM memory steel bars. The aim is to characterize the bond behavior, identify significant design parameters and to develop analytical models. In a first approach, the effects of different groove dimensions were investigated.

2 EXPERIMENTS

2.1 Materials

In this investigation, ribbed bars with a nominal bar diameter of 16 mm, delivered by company re-fer AG, were used. The rib geometry was according to British standard BS 6744:2001 (BSI 2009). The material offers high tensile strength of approximately $f_{u,mean}$=870 MPa at a failure strain of approximately $\varepsilon_{u,mean}$=30 %. The stress-strain behavior is illustrated in Figure 2. Detailed material properties can be found in (Michels et al. 2018).

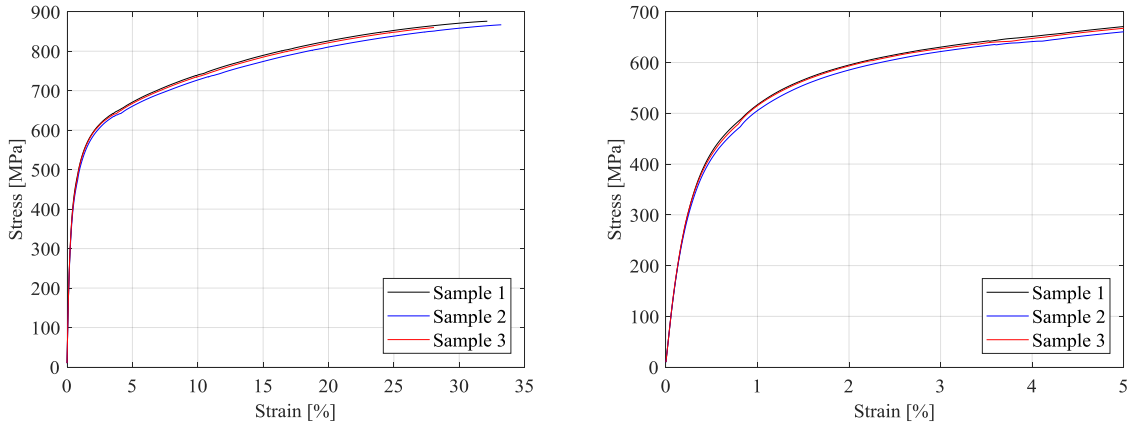

Figure 2. Full stress-strain curve of Fe-SMA bars 16 mm (left) and zoom-view up to 5 % strain (right)

A commercially available, shrinkage-compensated mortar, type Sika Grout 314 was used due to fast hardening and high compression strength. The bond-tests were performed after 36 days of mortar hardening which resulted in a compression strength of 94.4 MPa and bending-tensile strength of 6.3 MPa.
A concrete with maximum aggregate size of 32 mm and w/c-ratio of 0.5 was used. Mean compression strengths of 51.2 MPa and 56.7 MPa after 28 days and at the day of testing (56 days) were determined experimentally. Splitting tensile strength testing resulted in a tensile strength of 3.8 MPa after 28 days of hardening and 4 MPa at day of testing.

2.1.1 Manufacturing of concrete cube samples

The manufacturing process is depicted in Figure 3.The grooves were cut into the concrete cubes with a geometry of 200 x 200 x 200 mm using a dual-blade diamond saw (Step 1). The remaining concrete between the grooves was removed with a chisel (Step 2). The bond length of five times the bar diameter, or 80 mm, was ensured with two-part Styrofoam elements (Step 3). The memory steel bar installation and mortar casting process is illustrated in Figure 3 (Step 4). In this investigation, studies on six concrete cubes are presented. An overview of the performed tests is provided in Table 1.The groove depth and groove width were varied throughout the

tests. Therefore, three types of samples were manufactured with two samples each. Tests 1 and 2 had a groove depth of 27 mm (~1.5 d_b) and width of 34 mm (~2.0 d_b). The groove depth of 27 mm was considered to be realistic for a structure in outside conditions. The groove width of 2.0 d_b mm was chosen to enable good workability for the grouting process. Tests 3 and 4 had a groove depth of 51 mm (~3.0 d_b) and groove width of 34 mm (~2.0 d_b) to investigate the effects of deep embedment. Tests 5 and 6 had a groove depth of 27 mm (~1.5 d_b) and groove width of 51 mm (~3.0 d_b) to examine the effects of an increased groove width.

Figure 3. Cutting of slits (Step 1), Chiseling of remaining concrete (Step 2), Preparation for casting (Step 3), Casting of NSM pull-out samples (Step 4)

2.2 Test setup

The test setup is illustrated in Figure 4. A servo-hydraulic testing machine type Amsler with a maximum load capacity of 200 kN was used. The pull out test was performed in displacement control with an average rate of 0.008 mm/s. The pull-out load was recorded with a built-in load cell. The free-end slip was recorded with an LVDT. In addition, a digital image correlation system (DIC) of type ARAMIS by producer Gom was used to measure full-field deformations of the concrete surface. The measurement also enabled recording of slip of the bar at the load-free end for comparison with the LVDT measurement and slip of the bar on the load-side.

Figure 4. Front-view drawing of the pull-out test setup, dimensions in mm (left), illustrations of the pull-out test setup (right)

Table 1. Test matrix bond test campaign of bar diameter 16 mm.

No.	Groove depth h_g [mm]	Groove width w_g [mm]	Cover depth c [mm]	Max. stress in bar σ_{max} [MPa]	Max. bond stress $\tau_{m,max}$ [MPa]	Max. slip free-end $s_{max,fre}$ [mm]	Max. slip load-side $s_{max,ld}$ [mm]	Failure mode
1	~1.5 d_b 27 mm	~2.0 d_b 34 mm	9	271	13.5	0.14	0.22	I
2	~1.5 d_b 27 mm	~2.0 d_b 34 mm	9	250	12.6	0.16	0.25	I
3	~3.0 d_b 51 mm	~2.0 d_b 34 mm	33	382	19.2	0.21	0.51	II
4	~3.0 d_b 51 mm	~2.0 d_b 34 mm	33	340	17.0	0.25	0.40	II
5	~1.5 d_b 27 mm	~3.0 d_b 51 mm	9	251	12.6	0.21	0.29	I
6	~1.5 d_b 27 mm	~3.0 d_b 51 mm	9	285	14.3	0.15	0.25	I

3 RESULTS AND DISCUSSION

3.1 Definition of average bond stress and slip

Due to the limited bond length, an average bond stress was calculated by dividing the pull-out load by the nominal lateral surface of the bar. The free-end slip s_{fre} was measured with an LVDT. To obtain the slips on the free end and on the load-side s_{ld} of the bar from the DIC system, the average displacement of the concrete at the same longitudinal coordinate was subtracted from the displacement of the bar. Errors in the DIC measurement due to small out-of-plane rotations of the concrete blocks were considered in the analysis and led to a correction of obtained slips. As illustrated in Figure 5 (right), the DIC and LVDT measurement of the end-slip delivered approximately the same results.

3.2 Bond stress – slip behavior and failure modes

Figure 5 (left) shows the average bond stress - slip behavior of all samples. It is visible that tests 3 and 4 resulted in higher bond capacity and increased stiffness due to larger cover depth. Tests

1 and 2 show similar behavior as 5 and 6. Two primary failure modes were identified throughout the tests. Tests with small mortar cover (1, 2, 5, 6) failed in a brittle sudden manner without any residual frictional component. A cone-shaped tensile failure of the mortar cover and adjacent concrete occurred (see Figure 6, left), with full separation of the bar from the cementitious base material (Failure mode I). The failure was caused by high tensile stresses in the small cover and the high compression strength of the mortar, which prohibited shearing of the mortar substrate. As observable from the DIC measurement, transverse tensile stresses lead to longitudinal cracking of the mortar cover, already at low load levels. From the point where the cover is fully cracked longitudinally, the load further increases with lower stiffness until ultimate failure is initiated by wide-spread tensile cracking of mortar and adjacent concrete. The crack pattern of test 2 at maximum load level is illustrated in Figure 6 (center). The interface of mortar to concrete did not show any cracks at visual inspection. The mortar did not show significant signs of shear damage adjacent to the bar ribs due to high compression strength.

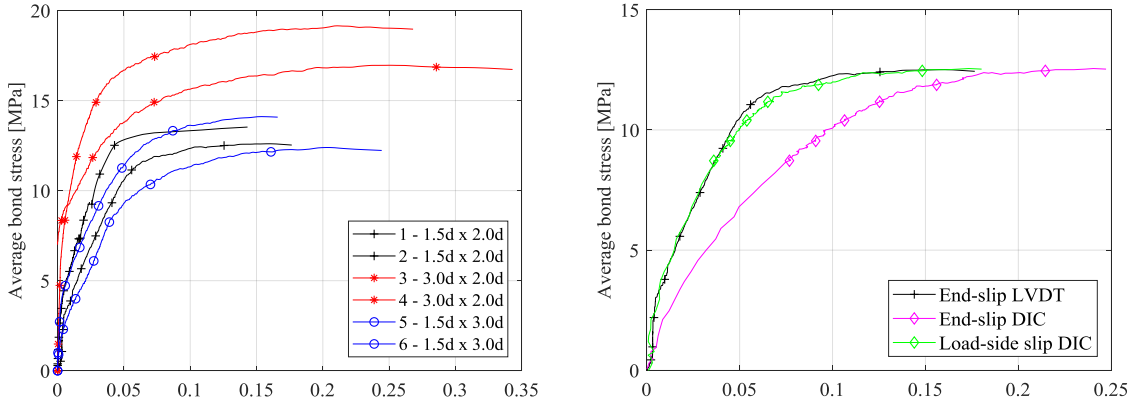

Figure 5. Average bond stress - end-slip curves pull-out tests (left), Comparison average bond stress –slip curves from LVDT and DIC measurement, test 2 (right)

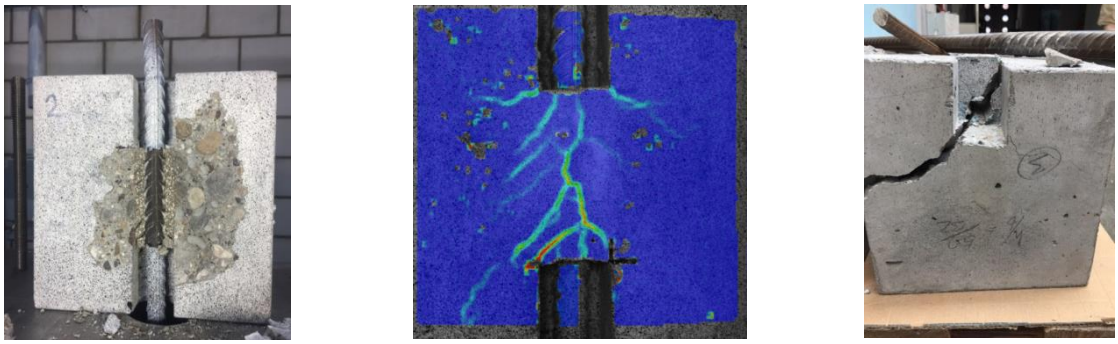

Figure 6. Failure mode I, representative for tests 1, 2, 5, 6 (left), Cracking visualized by DIC measurement at maximum load, test 2 (center), Failure mode II, representative for tests 3, 4 (right)

Tests 3 and 4 indicate a different failure mode and higher failure load. Tangential tensile stresses can be fully transferred by the increased mortar cover. However, the test results have to be analyzed with caution, since the sample failed by splitting of the whole concrete block (see Figure 6, right) (Failure mode II). Therefore the full capacity of the bonded joint could not be developed. It is assumed that with sufficient block geometry, the sample would fail by pull-out failure, meaning shearing of the mortar, adjacent to the ribs of the Fe-SMA bars. In this case, a load plateau, as well as a softening branch of the bond stress-slip curve would exist and residual friction would lead to a residual constant bond stress. Tests number 5 and 6 showed similar

behavior and failure mechanisms as tests 1 and 2, displaying brittle splitting failure. The load level, as well as slip did not deviate significantly from tests 1 and 2 with smaller groove width.

4 CONCLUSIONS AND OUTLOOK

Based on the current study, the following conclusions can be drawn:

1. Some experiments of a larger test campaign were presented, in which the bond behavior of Fe-SMA bars, known as memory steel bars, was investigated in a NSM configuration. The investigations focused on the influence of different groove dimensions. Even though the undesirable brittle failure mode splitting was observed, promising maximum average bond stresses of up to 13.5 MPa could be achieved in a low concrete cover configuration. This value is significantly higher than if the bond strength of conventional steel bars is estimated in normal-strength concrete with sufficient cover depth according to (Fédération Internationale du Béton 2012).
2. The failure mode and bond stress – slip behavior depends on the groove geometry, as expected. The groove depth and hence mortar cover has a large contribution to the behavior, whereas the groove width does not have a significant influence. The findings will be further investigated in ongoing investigations.
3. Even if the mortar cover is fully cracked longitudinally, the pull-out load further increases, however with decreased stiffness. The ultimate failure occurs in a cone-shaped tensile failure of mortar and adjacent concrete due to lateral compression forces.

Further design parameters, such as mortar strength, concrete strength, bar diameter, heating, prestress and bond length are under investigation in ongoing studies. To improve the soundness of the results, the number of sample size will be increased to three. The results will be used to define a simplified bond stress – slip law that serves as base for analytical bond modeling. Furthermore, research will focus on tests with full bond length, where the local bond stress-slip behavior will also be obtained with an alternative method and compared to current findings.

5 ACKNOLEDGEMENTS

This study was part of a PhD project, funded by the Swiss National Science Foundation (SNSF), number 200021_175998. The supply of materials by company re-fer AG is greatly appreciated.

6 REFERENCES

(2019). "re-fer AG product portfolio." Retrieved 10.02.2019, 2019, from https://www.re-fer.eu/systeme/re-plate/.

Abouali, S., M. Shahverdi, M. Ghassemieh, et al. (2019). "Nonlinear simulation of reinforced concrete beams retrofitted by near-surface mounted iron-based shape memory alloys." Engineering Structures 187: 133-148.

Asplund (1949). "Strengthening bridge slabs with grouted reinforcement." Journal of the American Concrete Institute 45(1): 397-406.

ASTM C234 (1991). Standard Test Method for Comparing Concretes on the Basis of the Bond Developed with Reinforcing Steel. Annual Book of ASTM Standards. 4.02: 153-157.

BSI (2009). "Stainless steel bars for the reinforcement of and use in concrete — Requirements and test methods." British Standards BS 6744:2001 + A2:2009: 28.

Czaderski, C., M. Shahverdi, R. Brönnimann, et al. (2014). "Feasibility of iron-based shape memory alloy strips for prestressed strengthening of concrete structures." Construction and Building Materials 56: 94-105.

De Lorenzis, L., A. Rizzo and A. La Tegola (2002). "A modified pull-out test for bond of near-surface mounted FRP rods." Composites Part B: Engineering 33(8): 589-603.

Fédération Internationale du Béton (2012). "Model Code 2010-Final draft, Volume 1. fib Bulletin, 65." Lausanne, Switzerland 1: 259-261.

Izadi, M., E. Ghafoori, A. Hosseini, et al. (2017). Feasibility of iron-based shape memory alloy strips for prestressed strengthening of steel plates. the fourth International Conference on Smart Monitoring, Assessment and Rehabilitation of Civil Structures (SMAR 2017).

Lee, H. Y., W. T. Jung and W. Chung (2017). "Flexural strengthening of reinforced concrete beams with pre-stressed near surface mounted CFRP systems." Composite Structures 163: 1-12.

Lee, W. J., B. Weber and C. Leinenbach (2015). "Recovery stress formation in a restrained Fe–Mn–Si-based shape memory alloy used for prestressing or mechanical joining." Construction and Building Materials 95: 600-610.

Meier, U. (1995). "Strengthening of structures using carbon fibre/epoxy composites." Construction and Building Materials 9(6): 341-351.

Michels, J., M. Shahverdi and C. Czaderski (2018). "Flexural strengthening of structural concrete with iron-based shape memory alloy strips." Structural Concrete 19(3): 876-891.

Michels, J., M. Shahverdi, C. Czaderski, et al. (2018). "Mechanical performance of iron-based shape-memory alloy ribbed bars for concrete prestressing." ACI Materials Journal 115(6): 877-886.

Michels, J., M. Shahverdi, C. Czaderski, et al. (2017). "Iron based shape memory alloy strips, part 2: flexural strengthening of RC beams." Proceedings of the SMAR.

Rehm, G. (1961). Über die Grundlagen des Verbundes zwischen Stahl und Beton, Deutscher Ausschuss für Stahlbeton, Heft 138, Berlin: Beuth Verlag.

RILEM TC (1994). Bond test for reinforcement steel. 2. Pull-out test. RILEM Recommendations for the Testing and Use of Constructions Materials. RILEM, SPON: 218-220.

Schranz, B. (2019). Ribbed iron-based shape memory alloy bars for pre-stressed strengthening applications. International Association for Bridge and Structural Engineering Symposium. Guimaraes, Portugal.

Schranz, B. (2019). Strengthening of concrete structures with iron-based shape memory alloy elements: Case studies. 5th International Conference on Smart Monitoring, Assessment and Rehabilitation of Civil Structures. Potsdam, Germany.

Sena-Cruz, J., J. Barros, V. Bianco, et al. (2016). "NSM Systems." 19: 303-348.

Shahverdi, M., C. Czaderski, P. Annen, et al. (2016). "Strengthening of RC beams by iron-based shape memory alloy bars embedded in a shotcrete layer." Engineering Structures 117: 263-273.

Shahverdi, M., C. Czaderski and M. Motavalli (2016). "Iron-based shape memory alloys for prestressed near-surface mounted strengthening of reinforced concrete beams." Construction and Building Materials 112: 28-38.

Shahverdi, M., J. Michels, C. Czaderski, et al. (2018). "Iron-based shape memory alloy strips for strengthening RC members: Material behavior and characterization." Construction and Building Materials 173: 586-599.

Windisch, A. (1985). "A modified pull-out test and new evaluation methods for a more real local bond-slip relationship." Materials and Structures 18(3): 181-184. The bond characteristics of the reinforcing steels are determined with the well known Pullout Test and/or Beam Test recommended by RILEM/CEB/FIP.